

# Thermal and Mechanical Properties of Carbon Nanotube/Epoxy Nanocomposites Reinforced With Pristine and Functionalized Multiwalled Carbon Nanotubes

Asad Hameed,<sup>1,2</sup> Mohammad Islam,<sup>2,3</sup> Iftikhar ahmad,<sup>3</sup> Nasir Mahmood,<sup>2,4</sup> Shaukat Saeed,<sup>5</sup> Hassan Javed<sup>6</sup>

<sup>1</sup>Department of Materials, University of Oxford, OX1 3PH, Oxford, UK

<sup>2</sup>School of Chemical and Materials Engineering (SCME), National University of Sciences and Technology (NUST), Islamabad 44000, Pakistan

<sup>3</sup>Center of Excellence for Research in Engineering Materials (CEREM), Advanced Manufacturing Institute, King Saud University, P.O. Box 800, Riyadh 11421, Saudi Arabia

<sup>4</sup>Department of Materials Science and Engineering, College of Engineering, Peking University, Beijing 100871, China

<sup>5</sup>Department of Metallurgy and Materials Engineering, Pakistan Institute of Engineering and Applied Sciences (PIEAS), Islamabad, Pakistan

<sup>6</sup>Department of Materials Science and Engineering, University of Erlangen Nuremberg, Martensstr. 5-7, Erlangen 91058, Germany

In this study, the effects of functionalization and weight fraction of multiwalled carbon nanotubes (CNTs) were investigated on mechanical and thermomechanical properties of CNT/Epoxy composite. Epoxy resin was used as matrix material with pristine-, COOH-, and NH<sub>2</sub>-functionalized CNTs as reinforcements in weight fractions of 0.1, 0.5, and 1.0%. Varying (increasing) the weight fraction and changing type (pristine or functionalized) of CNTs caused increment in Young's modulus and tensile strength as observed during mechanical tests. CNT reinforcement improved thermal stability of the nanocomposites as observed by thermogravimetric analysis. Thermomechanical analysis showed a slight reduction in free volume of the polymer, that is a drop in coefficient of thermal expansion, prior to glass transition temperature ( $T_g$ ) beside a slight increase in  $T_g$  value. Dynamic mechani-

cal analysis indicated an increase in storage modulus and  $T_g$  owing to the strength addition of CNT to the matrix alongside the hardener. Scanning electron microscopy analysis of the fractured surface(s) revealed that CNTs were well dispersed with no agglomeration and resulted in reinforcing the matrix. POLYM. COMPOS., 36:1891–1898, 2015. © 2014 Society of Plastics Engineers

## INTRODUCTION

Epoxy resins are widely used as matrix material owing to low shrinkage, excellent strength, chemical resistance, and processing versatility. Their inherent brittleness, tendency to delaminate, and low fracture toughness, however, limit their use, and thus necessitating incorporation and uniform dispersion of a tough second phase. Carbon nanotubes (CNTs) offer strong potential as a nanoscale filler material owing to their exceptional mechanical, electrical, and thermal properties coupled with high aspect ratio [1–3]. They exhibit tensile strength (TS) and elastic modulus in the range of 50–100 GPa and 1.4 TPa, respectively [4]. Nanocomposites are formed by CNT

---

Correspondence to: A. Hameed; e-mail:

asad.hameed@materials.ox.ac.uk or aerospace@hotmail.com

Contract grant sponsor: National University of Sciences and Technology (NUST), Islamabad.

DOI 10.1002/pc.23097

Published online in Wiley Online Library (wileyonlinelibrary.com).

© 2014 Society of Plastics Engineers

incorporation into the epoxy matrix to improve the physical properties of matrix. It is beneficial as there is no significant weight addition; in addition, the processing equipment required for such nanocomposites is the same as that used for neat resins. Although the CNT production cost is higher than that of conventional fillers, yet it is balanced out owing to low loading levels required.

Several challenges encountered while exploring CNTs as filler materials are (i) poor dispersion (in solvents/matrix) and tendency of forming agglomerates and bundles, (ii) low solubility in organic/inorganic solvents, (iii) low chemical reactivity with most species with a tendency to make weak bond(s), resulting poor interfacial strength, and (iv) the presence of impurities such as carbon soot/catalyst nanoparticles that undermine the properties of the final composites. Dispersion can be improved by employing a physical treatment such as ultrasonication, calendaring, ball milling, stirring, and extrusion [5] or through chemical modification process including oxidation, amidation, thiolation, silylation, halogenation, hydrogenation, and reaction with polymers [6]. It is noteworthy, however, that any treatment aimed at obtaining purification, good dispersion, and chemical reactivity must be performed with care owing to certain limitations and implications associated with its use. For example, ultrasonication can be carried out for low-viscosity liquids and prolonged exposure may induce structural damage to the nanotubes [7]. Similarly, extensive ball milling has been reported to decrease the CNT length [8] and low aspect ratio resulted in relatively less strong bond with the matrix [9].

Numerous researches have aimed at the development of epoxy/CNT nanocomposites primarily because of use of epoxy in high end applications such as aerospace industry. There are many reports on the effect of ultrasonic treatment, magnetic stirring, use of surfactants, and nanotube functionalization on the dispersion behavior of CNTs in the epoxy matrix [10–14]. The chemical functionalization is deemed an effective way of improving CNT dispersion and/or CNT–matrix bonding, which subsequently enhance the mechanical properties (TS, Young's modulus) and/or thermomechanical properties (glass transition temperature, storage, and loss moduli) of matrix [15–24]. Shen et al. [25] noticed an increase in thermal decomposition temperature with pristine CNTs having maximum effect and amine-functionalized nanotubes exhibiting the least effect on thermal stability enhancement. Compared with pristine nanotubes, functionalized CNTs had more significant effect on flexural strength and flexural modulus of the composites containing 0.2 wt% CNTs because of their strong interfacial bonding to matrix [26].

In this article, we present the results from chemical functionalization of CNTs for carboxylic ( $-\text{COOH}$ ) and amine ( $-\text{NH}_2$ ) groups attachment and subsequent incorporation into the epoxy in 0.1, 0.5, and 1.0 wt% loadings. The effectiveness of the functionalization treatment and the CNT dispersion into the epoxy was assessed by means

of FTIR and scanning electron microscopy (SEM) examination of the cryogenically fractured surface, respectively. After optimization of curing conditions, the effects of pristine/functionalized CNTs incorporation on the thermal and mechanical properties of the resulting composites were observed. From tensile testing of the specimens, experimental measurements of TS and Young's modulus were made. Change in the values of glass transition temperature, storage, and loss moduli, and coefficient of thermal expansion were determined using dynamic mechanical thermal analysis. Improvement in the thermal stability was deduced from thermogravimetric analysis of the neat and composite epoxy samples.

## EXPERIMENTAL

### Materials

The CNTs with an average diameter of  $\sim 50$  nm and length of the order of few microns were purchased from Sun Nanotech Company, China. The nanotubes were used either as-received (pristine- or P-CNT) or after chemical functionalization leading to attachment of carboxylic ( $-\text{COOH}$ ) or amine ( $-\text{NH}_2$ ) groups to the CNT surface; referred to as C–CNT or N–CNT, respectively. For purification and attachment of the functional groups, the chemical reagents such as hydrochloric acid (HCl), nitric acid ( $\text{HNO}_3$ ), sulfuric acid ( $\text{H}_2\text{SO}_4$ ), acetone ( $(\text{CH}_3)_2\text{CO}$ ), tetrahydrofuran ( $\text{C}_4\text{H}_8\text{O}$ ), thionyl chloride ( $\text{SOCl}_2$ ), ethylenediamine ( $\text{C}_2\text{H}_4(\text{NH}_2)_2$ ), and so forth with purity level of  $>99.99\%$  were procured from Sigma Aldrich and used without any further treatment.

The polymer matrix chosen for this study was commercially available epoxy resin (Araldite Ly-564) with hardener (Ardur Hy-2964). For tensile testing of the neat epoxy and composite specimens, a dog-bone mold was prepared on a computerized numerically controlled (CNC) horizontal milling machine (ENSHU, 500H) in accordance with ASTM D-638 standard, Type I.

### Covalent Functionalization of the Nanotubes

The covalent functionalization and subsequent characterization were carried out in the same way as described in our previous study [24]. Certain amounts of as-received CNTs were refluxed with HCl for 6 h at  $80^\circ\text{C}$  and then filtered. Then, an oxidative treatment in  $\text{H}_2\text{SO}_4$  and  $\text{HNO}_3$  mixed solution (1:3 v/v) was carried out by first thorough sonication for 2 h and then magnetic stirring at  $50^\circ\text{C}$  for 1 h. After a refluxing treatment at  $85^\circ\text{C}$  for 12 h, the mixture was thoroughly washed with distilled water until a pH of 7 was achieved. After drying at  $110^\circ\text{C}$  for 12 h, CNTs with attached hydroxyl ( $-\text{OH}$ ) and carboxylic ( $-\text{COOH}$ ) groups were obtained. Trace impurities from acidic treatments were removed by heating the dry residue at  $350^\circ\text{C}$  for 30 min in a furnace. Addition of carboxyl-functionalized nanotubes to  $\text{SOCl}_2$  sonication for 1 h, and finally, refluxing at  $60^\circ\text{C}$  for 24 h yielded acyl-

TABLE 1. Identification and description of neat epoxy and wt% CNT/epoxy samples.

| S.N | ID     | Degradation temp. (°C) |            |            |            |            | Thermal properties |                                    |                         | Mechanical properties |          |                  |
|-----|--------|------------------------|------------|------------|------------|------------|--------------------|------------------------------------|-------------------------|-----------------------|----------|------------------|
|     |        | $T_{10\%}$             | $T_{20\%}$ | $T_{30\%}$ | $T_{40\%}$ | $T_{50\%}$ | $T_g$ (°C)         | CTE ( $10^{-6}/^{\circ}\text{C}$ ) | $\tan \delta$ Peak (°C) | $E$ (GPa)             | TS (MPa) | $\epsilon_f$ (%) |
| 1   | E      | 381                    | 389        | 403        | 424        | 456        | 139.2              | 142                                | 153.8                   | ×                     | ×        | ×                |
| 2   | 0.1P/E |                        |            |            |            |            |                    |                                    |                         | +27.3                 | +13.7    | −6.2             |
| 3   | 0.5P/E | 382                    | 396        | 416        | 450        | 540        | 143.8              | 130                                | 155.5                   | +36.4                 | +16.6    | −14.2            |
| 4   | 1.0P/E |                        |            |            |            |            |                    |                                    |                         | +21.2                 | +10.6    | +6.4             |
| 5   | 0.1C/E |                        |            |            |            |            |                    |                                    |                         | +3.8                  | +10.1    | −3.6             |
| 6   | 0.5C/E | 382                    | 393        | 407        | 439        | 536        | 142.0              | 131                                | 154.6                   | +22.0                 | +15.7    | +10.7            |
| 7   | 1.0C/E |                        |            |            |            |            |                    |                                    |                         | +15.2                 | +24.2    | +15.8            |
| 8   | 0.1N/E |                        |            |            |            |            |                    |                                    |                         | +15.9                 | +16.3    | +5.0             |
| 9   | 0.5N/E | 383                    | 392        | 410        | 437        | 536        | 141.8              | 138                                | 154.8                   | +32.4                 | +16.6    | −18.1            |
| 10  | 1.0N/E |                        |            |            |            |            |                    |                                    |                         | +17.4                 | +31.4    | −12.6            |

E, epoxy (DGEBA); P, pristine CNT; C, COOH-functionalized CNT; N,  $\text{NH}_2$ -functionalized;  $T_g$ , glass transition temperature; CTE, coefficient of thermal expansion;  $E$ , elastic modulus; TS, ultimate tensile strength;  $\epsilon_f$ , engineering strain to fracture.

functionalized nanotubes with excess  $\text{SOCl}_2$  removed using  $\text{C}_4\text{H}_8\text{O}$ . After vacuum drying, the CNT powder was dispersed in  $\text{C}_2\text{H}_4(\text{NH}_2)_2$ , mixed ultrasonically for 6 h, and subsequently refluxed at  $85^{\circ}\text{C}$  for 48 h. Vacuum drying at  $80^{\circ}\text{C}$  followed by washing in ethanol, and drying at  $100^{\circ}\text{C}$  for 2 h produced amine-functionalized (N-CNT) nanotubes.

#### *Solution Mixing and Curing of Epoxy/CNT Nanocomposites*

Pristine or functionalized CNTs, in certain amount corresponding to 0.1, 0.5, or 1.0 wt%, were added to acetone. The resulting mixture was magnetically stirred for 15 min and sonicated at  $60^{\circ}\text{C}$  for 1 h in an enclosed container to prevent evaporation. Then, the acetone/CNT mixture was added to the heated epoxy resin and the solution was stirred at room temperature for 15 min followed by 1-h sonication at  $60^{\circ}\text{C}$ , remaining solvent (acetone) was evaporated at  $80^{\circ}\text{C}$  for 30 min. After adding the hardener in a certain ratio and stirring for 2 min, the mixture was transferred to a desiccator connected with vacuum pump for 5 min to remove air bubbles and the solvent, if present. The mold, precoated with release agent, was placed in the oven at  $80^{\circ}\text{C}$  with horizontal alignment checked using a water balance. CNT/epoxy mixture was poured into steel mold and cured first at  $80^{\circ}\text{C}$  for 1 h and later at  $140^{\circ}\text{C}$  for 2 h. After curing, the samples were extracted from the steel mold and mildly grinded (with 2,500 grit SiC paper) to remove surface nonconformities such as roughness, unevenness, kinks and sharp edges, and so forth Table 1 lists the sample identification and description for both neat and composite samples.

#### *Structural and Compositional Characterization*

HRTEM was performed using a Hitachi HNAR9000 microscope with accelerating voltage of 300 kV, LaB<sub>6</sub> electron gun, and 0.18-nm point-to-point resolution. Samples were prepared on the carbon grids by taking a droplet from the CNT dispersion in ethanol followed by drying in

air. Cryogenically fractured surfaces of various CNT/epoxy composites were examined under scanning electron microscope (JEOL JSM 6460). The information regarding chemical nature of the epoxy and nanocomposites surfaces was acquired using attenuation-total-reflection Fourier transform infrared spectroscope (ATR-FTIR) (JASCO FTIR-4100). A Thermogravimetric analyzer (TG/DTA) (TA Instruments Pyris 1 diamond Q5000IR) was used at a rate of  $10^{\circ}\text{C}/\text{min}$  in air to conduct thermal analysis of the nanocomposites.

#### *Mechanical Testing*

Tensile testing was carried out on a universal testing machine (TINIUS OLSEN 4465) at room temperature and crosshead speed of  $5 \text{ mm min}^{-1}$ . For each sample composition, at least three tests were performed. From the typical stress-strain curves, the values of Young's modulus ( $E$ ), TS, and engineering strain to failure ( $\epsilon_f$ ) were estimated and averaged out for each composition. For dynamic mechanical thermal analysis studies, the specimens were made as thin sheets with approximate dimensions  $\sim 20 \times 2.5 \times 0.3 \text{ mm}$  and tested on Perkin Elmer TMA Q400 at a frequency and heating rate of 1 Hz and  $5^{\circ}\text{C min}^{-1}$ , respectively, when heated from  $\sim 90$  to  $170^{\circ}\text{C}$ .

## RESULTS AND DISCUSSION

#### *Chemical, Compositional, and Morphological Characterization*

The chemical formula for diglycidyl ether of bisphenol-A (DGEBA) and the FTIR spectra of the resin, hardener, and cured neat epoxy (DGEBA) are shown in Fig. 1. Although the absorption band positioned at  $913 \text{ cm}^{-1}$  is identified to be owing to the epoxy group, the bands at 1,140, 1,356, 2,870, and  $3,485 \text{ cm}^{-1}$  are characteristic of C=C groups, N—H bending vibrations, alkyl groups, and N—H stretching mode vibrations, respectively, from the hardener which is a cyclo-polyaliphatic amine. After the resin was mixed with the hardener and the blend thermally



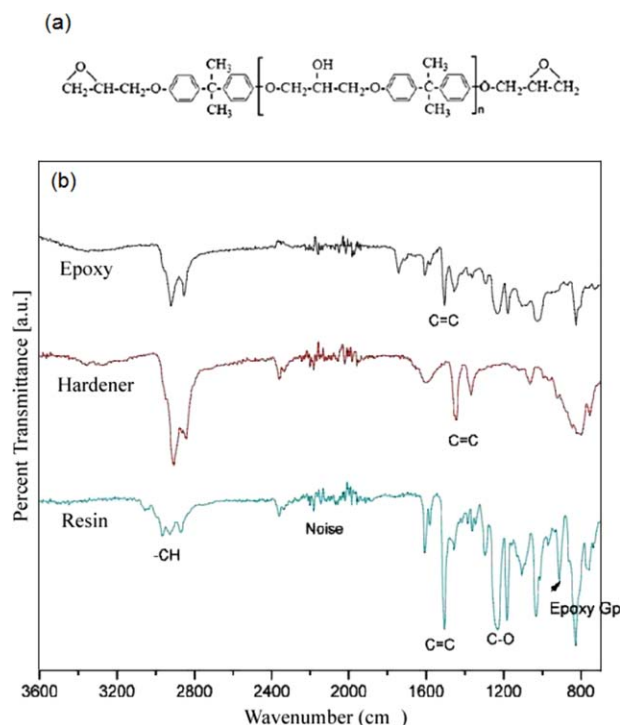


FIG. 1. (a) Molecular structure of DGEBA epoxy and (b) FTIR spectra of resin, hardener, and cured neat epoxy. [Color figure can be viewed in the online issue, which is available at [www.interscience.wiley.com](http://www.interscience.wiley.com).]

cured, the intensity of the absorption band for the epoxy group ( $913\text{ cm}^{-1}$ ) diminished owing to the consumption of most of the epoxy groups during curing treatment. Upon incorporation of CNTs, whether pristine or functionalized, no noticeable change in FTIR spectra was observed. It is primarily owing to very small weight fraction of nanotubes used for reinforcement. Another possible reason is that the peaks arising from O—H, C=C, C—O, and N—H groups are already present in the neat DGEBA epoxy [24].

The modification of CNT structure after the acid purification and treatment is confirmed from HRTEM examination as shown in Fig. 2. The multiwalled structure formed by concentric graphene shells is evident from the high-magnification side view of an individual CNT with an intershell spacing of 0.34 nm. Treatment with HCl and then with  $\text{H}_2\text{SO}_4 + \text{HNO}_3$  solution caused the removal of catalyst nanoparticles and other carbonaceous deposits from CNT powder. The formation of  $\sim 1.8\text{-nm}$ -thick amorphous layer adjacent to the outermost CNT shell is noticed. Acid treatment adversely affected the lattice structure as evident from rupture of the few coaxial shells at and near the nanotube side wall (Fig. 2b). It is anticipated that subsequent treatment with thionyl chloride and ethylenediamine may cause more damage to the nanotube structure.

### Thermal Properties

Thermal stability of the composite epoxy samples was assessed using TGA for epoxy composites with 0.5 wt% loading of pristine-, carboxylic-, or amine-functionalized

CNT and compared with thermal properties of the neat epoxy. The decomposition behavior as a function of temperature is graphically shown in Fig. 3. Although the temperature indicative of the onset of thermal degradation is the same that is  $\sim 370^\circ\text{C}$  for all the samples, nanotube incorporation led to enhanced thermal stability, assessed from their per cent weight loss with respect to temperature (Table 1). Neat epoxy underwent 50% weight loss upon heating to  $456^\circ\text{C}$ , for 0.5 wt% CNT/epoxy samples similar degree of degradation, was experienced at higher temperature ( $\sim 540^\circ\text{C}$ ). This is owing to the fact that pristine CNTs are more thermally stable owing to their defect-free, crystalline structure in comparison with functionalized (COOH or  $\text{NH}_2$ ) CNTs. Higher temperatures corresponding to the similar extent of decomposition are observed for 0.5P/E samples in comparison with 0.5C/E or 0.5N/E samples. The temperatures corresponding to different degrees of weight loss (%) for various samples are listed in Table 1.

From TMA studies, the change in (length) dimension upon increasing the temperature was recorded as shown in Fig. 4. The coefficient of linear thermal expansion (CTE) for each composition was computed by determining the slope of the linear segment of the graph prior to glass transition range. The value of CTE decreased ( $142\text{ }\mu\text{m }^\circ\text{C}^{-1}$  for neat epoxy) to a minimum value of  $131\text{ }\mu\text{m }^\circ\text{C}^{-1}$  for 0.5C/E composite sample which may be attributed to

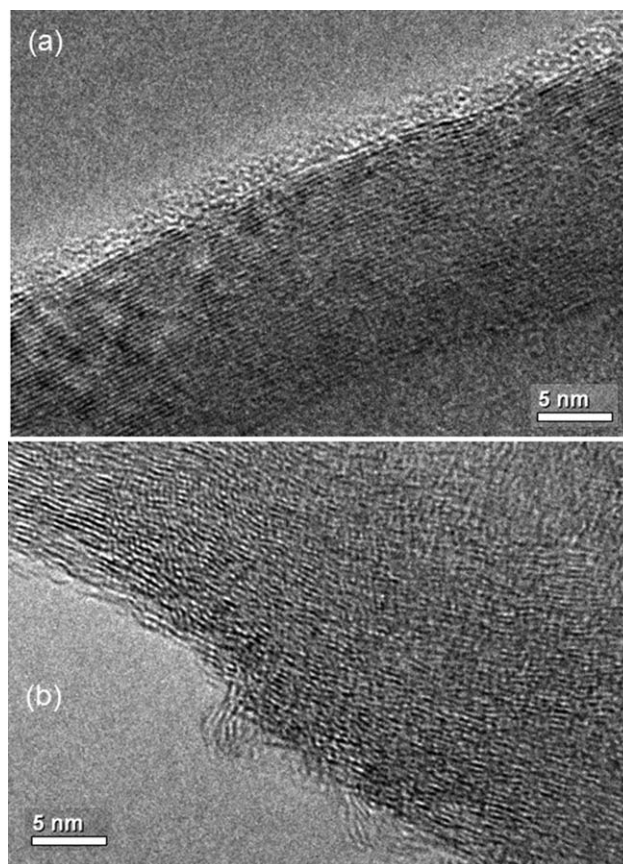


FIG. 2. HR-TEM microstructures of CNT after: (a) Purification with HCl and (b) treatment with  $\text{H}_2\text{SO}_4 + \text{HNO}_3$ .

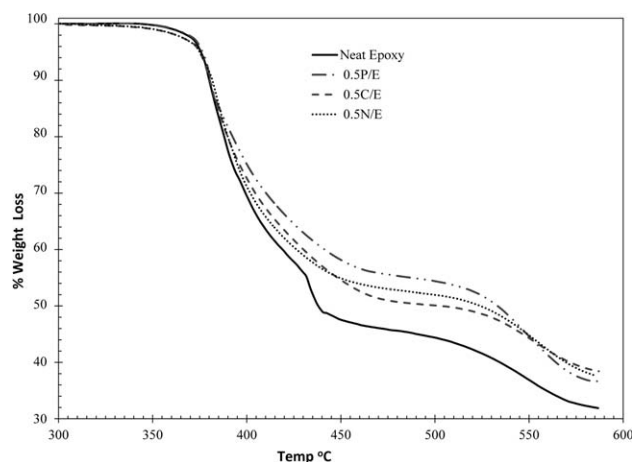


FIG. 3. TGA weight loss data over a range of temperatures for neat epoxy and nanocomposite samples.

restraining effect of the nanotubes upon heating. A typical TMA curve shows a linear section on either side of the glass transition, indicating expansion below and above the glass transition temperature ( $T_g$ ). The value of  $T_g$  for each case was determined at the point where the extrapolated lines before and after the glass transition intersect (Fig. 4). The findings indicate an increase in  $T_g$  value upon CNT incorporation with the maximum value obtained for 0.5C/E composite. The findings invariably point out to the fact that thermal properties improve by the addition of pristine CNTs, whereas rheological properties enhance upon addition of the functionalized CNTs owing to the strong adhesion of the matrix with the CNTs through a covalent interaction. The values of CTE and  $T_g$  for the neat epoxy and nanocomposite samples containing 0.5 wt% of any type of the CNT are listed in Table 1.

### Mechanical Properties

During DMA studies, the change in storage modulus ( $E'$ ) was recorded against temperature at a frequency of 1.0 Hz. For neat epoxy and nanocomposite samples containing 0.5 wt% of pristine-, carboxylic- or amine-functionalized CNT, the data plots for storage modulus (logarithmic scale) and dissipation factor (also called  $\tan \delta$ , the ratio of loss modulus to storage modulus, i.e.  $E''/E'$ ) versus temperature are shown in Fig. 5. From the semi-log  $E'-T$  plot (Fig. 5a), the onset of glass transition was determined at the point where a large drop in the  $E'$  value occurred. The  $T_g$  values obtained for neat epoxy and 0.5P-CNT/E samples were found to be  $\sim 141.5$  and  $147^\circ\text{C}$ , respectively. From comparison of the two samples, it is evident that CNT incorporation minimizes contributions by localize chain movements and bending/stretching of chains toward drop in  $E'$  during initial heating. The nonlinear behavior at low temperatures probably originates from distribution of length scales or inhomogeneities and rearrangement of particles or filaments used as fillers. There is an associated rise in the position of rubbery plateau indicative of chain motion over a large length scale.

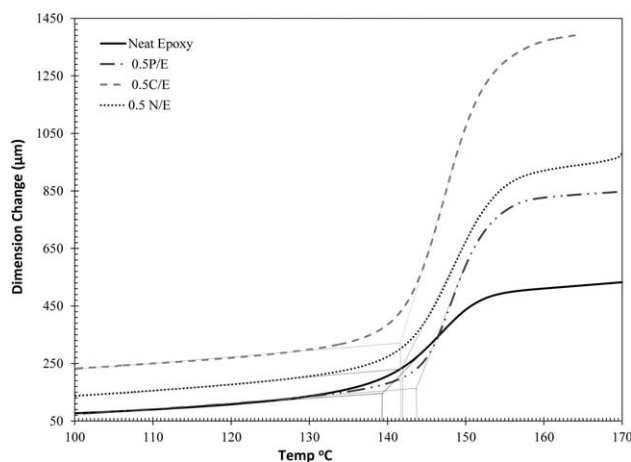


FIG. 4. Dimensional change as a function of temperature for pure epoxy and different epoxy/CNT composites.

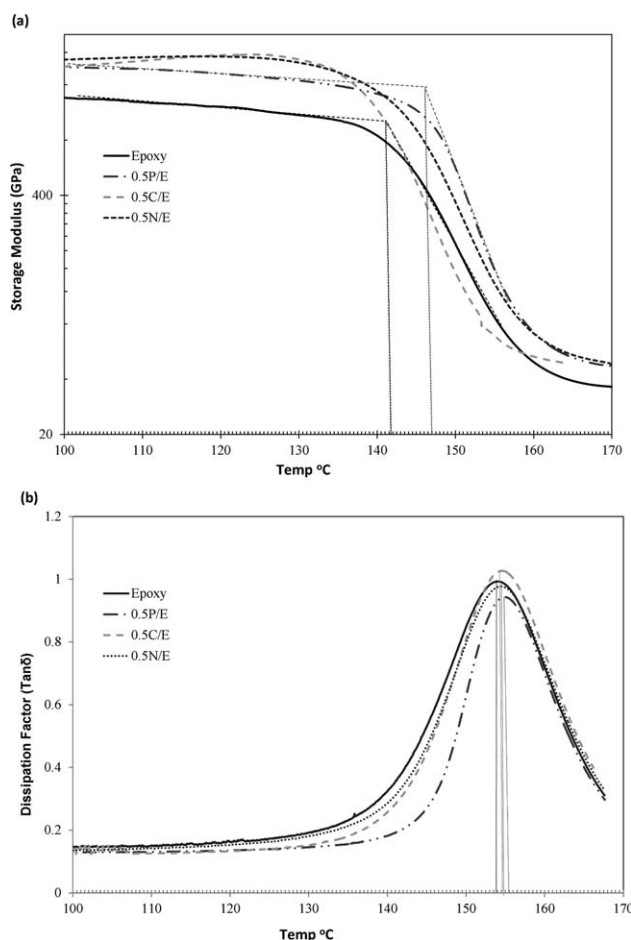


FIG. 5. DMA studies of neat epoxy and different CNT/E composites for a range of temperatures at 1.0 Hz frequency and  $5^\circ\text{C}/\text{min}$  heating rate: (a) storage modulus and (b) dissipation factor ( $\tan \delta$ ).

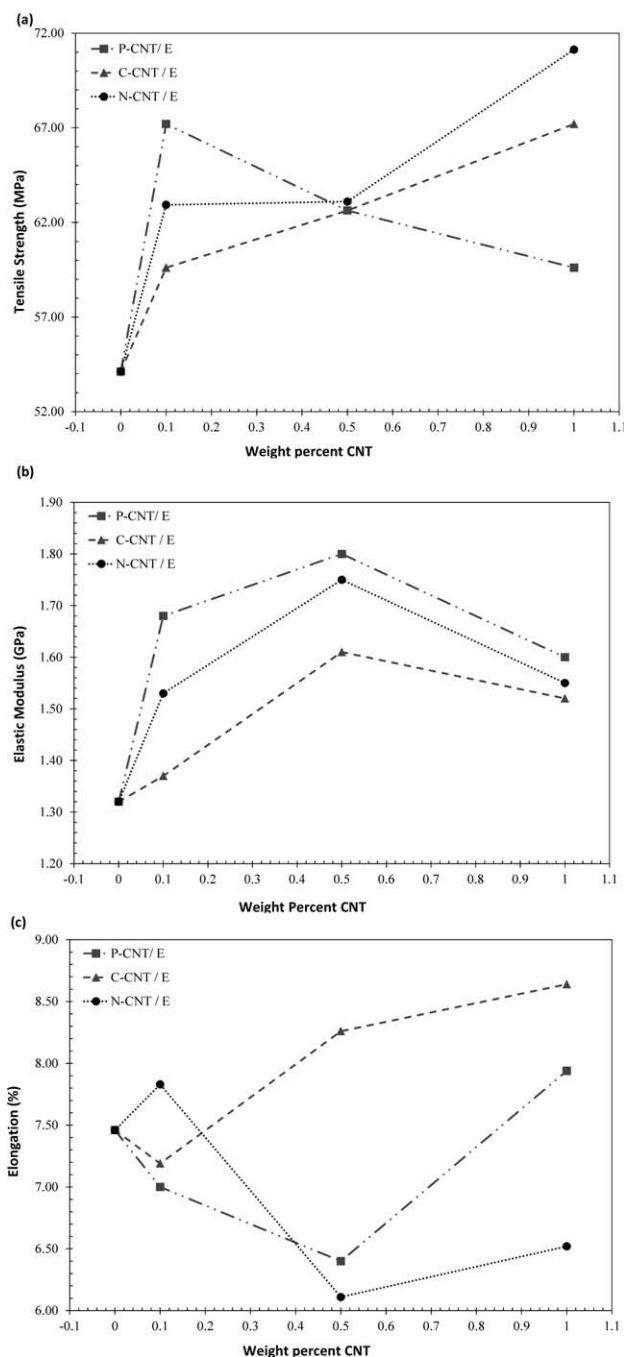


FIG. 6. Mechanical properties of neat and composite epoxy samples with 0.5 wt% CNT: (a) elastic modulus, (b) TS, and (c) strain to failure.

Nevertheless, all the composite samples exhibited a higher  $E'$  value than that of neat epoxy. As shown in Fig. 5b, CNT addition to epoxy resulted in more homogeneous structure as manifested by reduced width of the dissipation factor peak for all composite samples. As the extent of reduction in peak width was the greatest for 0.5P/E composition, incorporation of pristine CNT had most prominent effect on homogeneity. Except for 0.5C/E, all the composite samples experienced a drop in maximum  $\tan \delta$  value, indicating a shift toward more elastic nature of the samples. The

obtained  $T_g$  values were slightly higher than those obtained from TMA.

The data were obtained from tensile testing of the dog-bone specimens made from neat epoxy as well as nanocomposites incorporating 0.1, 0.5, or 1.0 wt% of pristine-, carboxylic-, or amine-functionalized CNT show interesting trends, as depicted in scatter-line charts shown in Fig. 6. Compared to pure epoxy, all the composite compositions exhibit an increase in the values of elastic modulus ( $E$ ) and TS. Although the  $E$ -value peak upon addition of 0.5 wt% CNT regardless of nanotubes type followed by a decrease, the TS values maximize in case of 1.0 wt% C or N-CNT. The extent of improvement in  $E$ -value was maximum for 0.5P/E composition perhaps owing to superior crystallinity and structural integrity of pristine nanotubes as compared to their functionalized CNT-reinforced counterparts which undergo shortening and defect formation during chemical functionalization. A drop in  $E$ -value upon further increase in CNT content to 1.0 wt% is probably owing to nanotube agglomeration, leading to nonhomogeneous dispersion within epoxy matrix. On the other hand, generation of defects on nanotubes sidewalls as well as attachment of functional groups

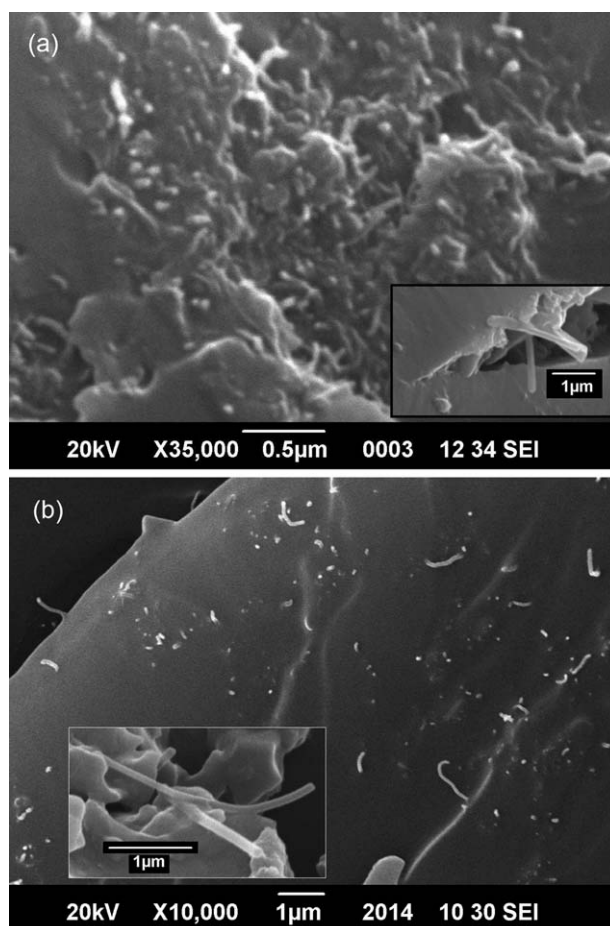


FIG. 7. SEM microstructures of the cryogenically fractured surfaces of nanocomposite samples: (a) 0.5P/E and (b) 0.5N/E. The insets show CNT-based filaments protruding out of epoxy matrix.



improved CNT/epoxy interfacial strength through covalent bonds among the functional groups present on CNTs surface and oxygenated groups of epoxy, as manifested by a significant increase in TS value for 1.0N/E and 1.0C/E composites. It is possible that, in case of 1.0P-CNT, the extent of CNT agglomeration is on a larger scale as evident from a decrease in TS for the composition. The per cent increase in the values of  $E$ , TS, and  $\varepsilon_f$  with respect to neat epoxy sample is summarized in Table 1.

The comparison of fractured surfaces for 0.5P/E and 0.5N/E nanocomposites is made through SEM examination as shown in Fig. 7. In case of pristine CNT incorporation, bright dots and strands are observed which represent CNT rupture and CNT pullout from epoxy matrix, respectively. The length of the CNT segment pulled out of epoxy is of the order of 1  $\mu\text{m}$  or less. This implies that, in the absence of any surface modification of CNT, the specimen fails without very efficient load transfer to the reinforcing nanotubes. The inset in Fig. 7a shows propagation of a crack along with pullout of CNT from epoxy in the process. As the outer diameter of the dangling fiber is  $\sim 170$  nm, almost three times higher than the average CNT diameter, the failure seems to have occurred within the epoxy matrix. Figure 6b shows that while addition of 0.5N-CNT improved dispersion, the fracture is predominantly brittle as evident from the smooth, flat morphology of the fractured surface. In case of 0.5N-CNT/E composition, the outer diameter and length of the individual nanotubes, de-bonded from the matrix, is noticed to be  $\sim 122$  nm and few microns, respectively. It is speculated that higher interfacial strength causes higher degree of fiber/nanotubes pullout and a relatively low value of filament diameter.

## CONCLUSIONS

Chemical functionalization of CNT sidewalls improves adhesion of epoxy through covalent interactions, and thus leading to effective load transfer during tensile testing. Extensive chemical treatment, however, deteriorates thermal stability through increased defect density. Nanocomposites exhibited varying degrees of enhanced thermal properties in comparison with the neat epoxy in terms of higher values for onset of degradation temperature, higher values of  $T_g$ , and lower values of CTE prior to  $T_g$ . Although nanotube incorporation, whether pristine or functionalized, caused various degrees of improvement in mechanical properties (elastic modulus and TS), maximum per cent increase was noticed for nanocomposites with 0.5 wt% nanotubes which may be attributed to good dispersion and strong interfacial bonding between nanotube surface and the epoxy. Although tensile properties of nanocomposites with 1.0 wt% CNT are still superior to that of neat epoxy, increase in  $E$ -values slightly dropped probably owing to nanotube agglomeration within epoxy matrix. On the other hand, TS values maximize for 1.0 wt% loading owing to the combined effects of

nanotube disentanglement and effective load transfer. Among different types and loading levels of CNTs explored, nanocomposites containing 0.5 wt% amine-functionalized CNTs offer the best combination of thermal and mechanical properties with slight compromise on strain to fracture. The fracture surfaces with features such as length and outer diameter of pulled-out filaments from epoxy matrix are good indicators of load transfer and load-bearing characteristics of reinforcing nanotubes.

## ACKNOWLEDGMENT

The authors appreciate assistance in HR-TEM studies from Mr. Nicolas Gautier at Institut des Materiaux (IMN), Universite de Nantes, France. M. Islam is also thankful to the French government for the postdoctoral research fellowship awarded through the French embassy in Islamabad, Pakistan.

## REFERENCES

1. J.P. Lu, *Phys. Rev. Lett.*, **79**, 1297 (1997).
2. J.P. Salvetat, G.A.D. Briggs, J.M. Bonard, R.R. Bacsá, A.J. Kulik, T. Stöckli, N.A. Burnham, and L. Forró, *Phys. Rev. Lett.*, **82**, 944 (1999).
3. E.T. Thostenson, C. Li, and T.W. Chou, *Compos. Sci. Technol.*, **65**, 491 (2005).
4. Y. Zhou, F. Pervin, L. Lewis, and S. Jeelani, *Mater. Sci. Eng. A*, **475**, 157 (2008).
5. P.C. Ma, N.A. Siddiqui, G. Marom, and J.K. Kim, *Compos. A: Appl. Sci. Manufact.*, **41**, 1345 (2010).
6. A. Hirsch and O. Vostrowsky, "Functionalization of Carbon Nanotubes," in *Functional Molecular Nanostructures*, Springer, Berlin/Heidelberg, 193 (2005).
7. S. Bal and S. Samal, *Bull. Mater. Sci.*, **30**, 379 (2007).
8. M. Endo, H. Muramatsu, T. Hayashi, Y. Kim, M. Terrones, and M. Dresselhaus, *Nature*, **433**, 476 (2005).
9. A.M. Esawi and M.M. Farag, *Mater. Design*, **28**, 2394 (2007).
10. X. Gong, J. Liu, S. Baskaran, R.D. Voise, and J.S. Young, *Chem. Mater.*, **12**, 1049 (2000).
11. S. Cui, R. Canet, A. Derre, M. Couzi, and P. Delhaes, *Carbon*, **41**, 797 (2003).
12. J.A. Kim, D.G. Seong, T.J. Kang, and J.R. Youn, *Carbon*, **44**, 1898 (2006).
13. J. Qiu, C. Zhang, B. Wang, and R. Liang, *Nanotechnology*, **18**, 095708 (2007).
14. W. Chen, M.L. Auad, R.J. Williams, and S.R. Nutt, *Eur. Polym. J.*, **42**, 2765 (2006).
15. G. Gkikas, N.M. Barkoula, and A. Paipetis, *Compos. B: Eng.*, **43**, 2697 (2012).
16. S.H. Hsu, M.C. Wu, S. Chen, C.M. Chuang, S.H. Lin, and W.F. Su, *Carbon*, **50**, 896 (2012).
17. M. Rahman, S. Zainuddin, M. Hosur, J. Malone, M. Salam, A. Kumar, and S. Jeelani, *Compos. Struct.*, **94**, 2397 (2012).
18. I. Srikanth, S. Kumar, A. Kumar, P. Ghosal, and C. Subrahmanyam, *Compos. A: Appl. Sci. Manufact.*, **43**, 2083 (2012).

19. Y. Luo, Y. Zhao, J. Cai, Y. Duan, and S. Du, *Mater. Design*, **33**, 405 (2012).
20. Q. Zehua and W. Guojian, *J. Appl. Polym. Sci.*, **124**, 403 (2012).
21. C. Damian, S. Garea, E. Vasile, and H. Iovu, *Compos. B: Eng.*, **43**, 3507 (2012).
22. L. Guadagno, B. De Vivo, A. Di Bartolomeo, P. Lamberti, A. Sorrentino, V. Tucci, L. Vertuccio, and V. Vittoria, *Carbon*, **49**, 1919 (2011).
23. L.J. Cui, Y.-B. Wang, W.J. Xiu, W.Y. Wang, L.H. Xu, X.B. Xu, Y. Meng, L.Y. Li, J. Gao, and L.T. Chen, *Mater. Design* (2013).
24. N. Mahmood, M. Islam, A. Hameed, S. Saeed, and A.N. Khan, *J. Compos. Mater.*, **48**, 1197 (2014).
25. J. Shen, W. Huang, L. Wu, Y. Hu, and M. Ye, *Compos. Sci. Technol.*, **67**, 3041 (2007).
26. J. Kathi, K.-Y. Rhee, and J.H. Lee, *Compos. A: Appl. Sci. Manufact.*, **40**, 800 (2009).